Observation of Single-Particle Plasmons by Near-Field Optical Microscopy

U. Ch. Fischer[(1)] and D. W. Pohl[(2)]

[(1)]*Ernst-Leitz-GmbH, D 6330 Wetzlar, Federal Republic of Germany*

[(2)]*IBM Research Division, Zurich Research Laboratory, 8803 Rüschlikon, Switzerland*[(a)]

(Received 12 October 1988)

Plasmons in small protrusions of an otherwise flat gold film were studied with a scanning near-field optical microscope (SNOM). Individual protrusions were selected by approaching them with another medium in a controlled way. Extremely narrow resonances in terms of scattering intensity versus distance were observed. The results open new opportunities for local plasmon studies as well as for SNOM with enhanced sensitivity and resolution, e.g., operation in a novel topographic mode (optical tunnel microscopy).

PACS numbers: 73.20.Mf, 07.60.Pb, 72.10.Fk

Surface plasmon (SP) excitations in small particles and protrusions (< 100 nm in diameter) play an important role for the optical properties of rough or otherwise microscopically structured metal surfaces.[1] SP's drew particular attention in the context of surface-enhanced Raman scattering.[2] Experimental SP studies so far, to our knowledge, have been restricted to large ensembles of particles or protrusions,[1] yielding information on average optical properties rather than on truly microscopic ones.

The new noncontact stylus microscopies such as scanning tunneling and scanning near-field optical microscopy (STM[3] and SNOM[4-8]) have shown new ways for manipulation and characterization which are sufficiently local to study *individual nanometer-size structures.* In SNOM, the radiation from a subwavelength-size probe light source (optical antenna) is recorded while the sample (object) is approached or raster scanned in immediate proximity of the antenna. A resolution far beyond the diffraction limit ($\simeq 20$ nm for visible light[4,5]) was achieved with this method.

We wish to report here on the first observation of SP's by SNOM, their dependence on particle size, and their response to a change of particle environment; we also show how these properties can be exploited to enhance the sensitivity of SNOM and operate it in a novel topographic mode, "optical tunneling," which is strictly analogous to constant-current STM.[3]

The "antenna" of the present SNOM is a small, illuminated protrusion of, roughly, 50 to 150 nm in diameter on an otherwise flat gold film [Fig. 1(a)]. The experimental setup is a simple modification of the recently reported reflection SNOM[9] with the protrusion in place of the probe aperture [Fig. 1(a)]. The protrusions are formed by polystyrene particles nominally 90 nm in diameter, adsorbed on a microscope slide at a mean distance of several 10 μm. Both glass and particles are covered with a 20-nm-thick gold film. Prism couplers feed light from a HeNe laser in and out of the slide, traversing its length on a zigzag path and illuminating the film as in the Kretschmann configuration for thin-film SP investigations[1] and a recently proposed surface-enhanced Raman scattering microscope.[10] The antenna radiation from the selected protrusion produces "scattered" or "stray" light, part of which is collected by an auxiliary microscope.[9] With the chosen density of polystyrene spheres, it is easy to focus the auxiliary microscope on a particular one and record its individual radiation intensity I_s with a photomultiplier attachment.

The objects in the first part of the investigation were small convex glass lenses whose curvature facilitates approach to the probe. The object support, consisting of a combination of manual micrometers and piezoelectric elements, allows rough and fine positioning in all three dimensions as well as raster scanning, very similar to an STM.

To study the possibility of SP excitation, we recorded I_s as a function of sample position z_s, while the probe was kept in a fixed position $z_p \simeq 0$. The angle of incidence θ was chosen to cover the relevant part of the thin-film SP dispersion curve.[1] Further, the polarization was switched between p and s orientation with the expectation that SP effects would predominantly occur in the p mode.[1] Several probe slides were prepared; on each of

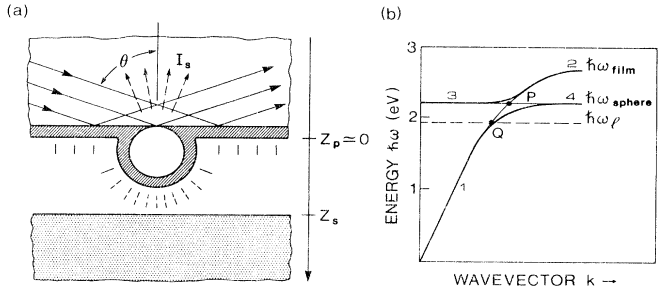

FIG. 1. (a) SNOM probe and sample arrangement. (b) Plasmon dispersion curves (schematic) for flat thin film (1-*P*-2), small sphere (3-*P*-4), and hybrid modes (1-4,3-2).

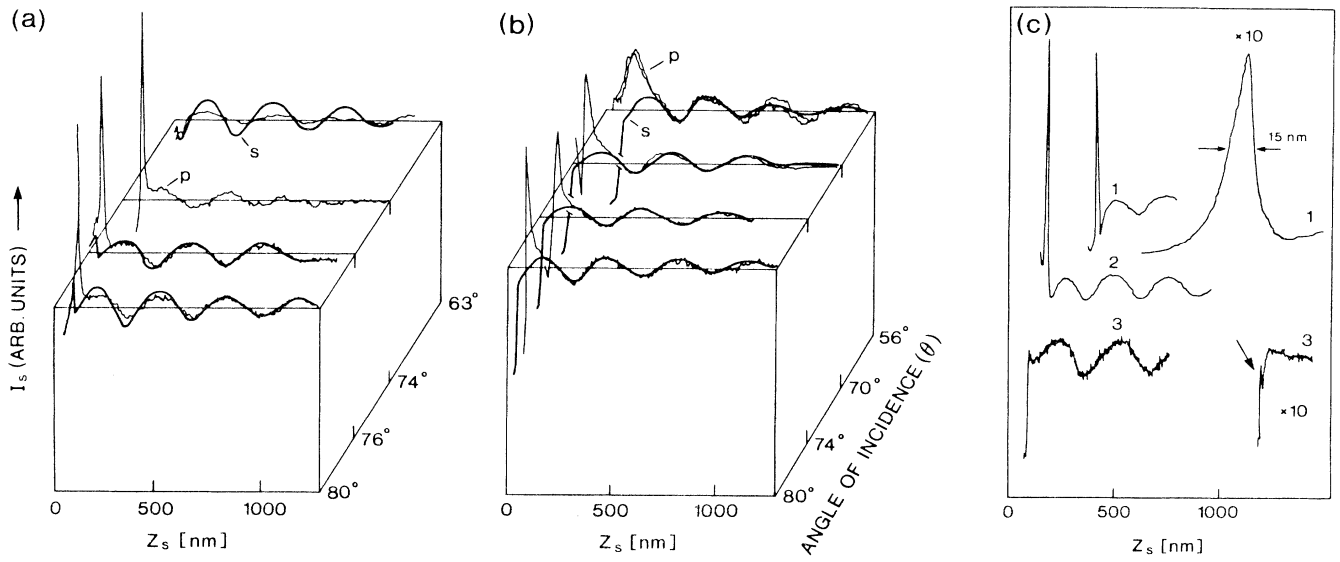

FIG. 2. Light scattering intensity $I_s(z_s)$ during probe-sample approach for typical scatterers [(a),(b) including angular dependence; (c) extreme cases].

them a number of scattering centers were studied. The approaching motion was stopped when I_s had become considerably smaller than the average value at a large distance $\langle I_s \rangle$. The signal was quite reproducible under these conditions.

Figure 2 shows three sets of results. Coming from a large distance z_s, interference undulations are observed as in previous aperture SNOM experiments.[9] For p polarization, an *additional strong narrow peak* shows up which obviously differs from the interference maxima. For s polarization [Figs. 2(a) and 2(b), "s" curves slightly smoothed for distinction] the additional peak is missing—a first indication that (thin film) SP's[1] may be involved. To the left of the peak one frequently notices a sharp kink which is of minor interest here; it might be caused by physical contact or capillary condensation of a water bridge.[11] The interference may be caused by the Fabry-Perot-type arrangement of the probe slide and the sample surface, and hence a measure for the gap width $z_s - z_p$. Depending on the somewhat uncertain effective optical constants, contact is calculated to occur 200 to 300 nm after passage through the last interference maximum.

The peaks of Fig. 2(a) have heights $I_s^{\text{peak}} \simeq \langle I_s \rangle$ (background subtracted), and a full width at half maximum (FWHM) < 20 nm. They occur for very shallow incidence only, $\theta > 63°$—another hint of (thin film) SP.[1] Figure 2(b) shows the results from a stronger scatterer (larger $\langle I_s \rangle$), providing broad asymmetric peaks of small height, coming immediately after the last interference maximum. The FWHM clearly depends on θ, with a heavily broadened peak for the steepest incidence. The latter trace was repeated twice to demonstrate the reproducibility of the data. Figure 2(c) depicts three other interesting approach curves: (1) a peak riding right on the slope of the undulation with an FWHM of only 15 nm, (2) the tallest peak, and (3) the narrowest one observed with an FWHM of 1–3 nm (recognizable only on the extended-scale display) from a very weak scatterer. For calibration and comparison, the approach experiments were repeated with a glass surface covered with 5 nm of W/Ta film as the sample. No peak or just a faint indication of a peak was found in this case while the interference pattern was more pronounced than before, as is to be expected for a highly reflecting object.

In Fig. 3, the FWHM and I_s^{peak} of the entire series of measurements are plotted as a function of peak position. The various symbols refer to different orientations θ of the incident laser beam. The distance $\Delta z = z_s^{\text{peak}} - z_s^{\text{max}}$ from the peak to the last interference maximum was chosen as a measure of position. Although the parameters FWHM, I_s^{peak}, and Δz could not be determined with high precision (see error bars), one notices a distinct trend for the FWHM to increase when the peak position gets closer to z_s^{max}. The peak height, on the other hand, appears to have a maximum in the range -180 nm $< \Delta z < -140$ nm. Both sets of data points extrapolate to zero for $\Delta z \simeq -220$ nm. The influence of θ, obvious in Figs. 2(a) and 2(b) and reflected by data points on the right-hand side of Fig. 3, seems to be insignificant for more negative values of Δz.

For a qualitative interpretation of the experimental results, we consider the hybrid plasmon modes of the system of a *flat thin film and small sphere.* Figure 1(b) schematically shows the respective dispersion relation. Branches 1 and 2 represent the propagating thin-film modes while 3 and 4 are associated with the dispersion-free lowest-order spherical mode.[1] The limiting frequen-

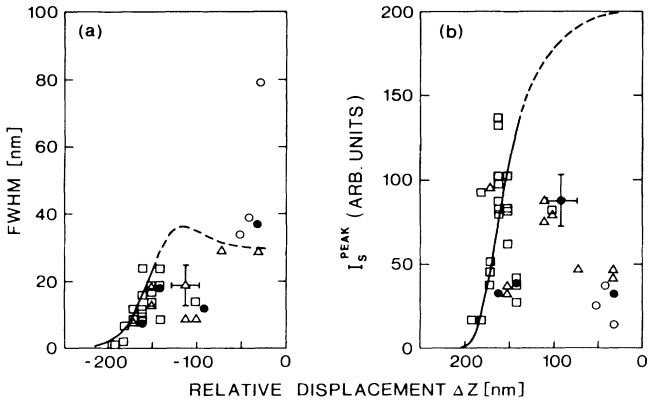

FIG. 3. (a) FWHM and (b) peak height of the resonances as a function of position of scatterers ($\theta < 72°$: ○; 72°–76°: ● 75°–80°: □; $> 80°$: △).

cies for a gold film adjacent to air are $\hbar\omega_{\text{film}} \simeq 2.7$ eV and $\hbar\omega_{\text{sphere}} \simeq 2.2$ eV.[1] The shape of the coupled-mode curves (heavy lines) follows from the known rules of wave interaction. Enhanced radiation from the probe sphere requires the excitation of a particlelike SP, residing near the flat parts 3 or 4. Effective coupling to the incident light wave, on the other hand, favors a point on the 1 and 2 branches because of the larger interaction area. Optimum conditions therefore may be expected near the crossover point P.

The energy of He-Ne laser photons, $\hbar\omega_l = 1.96$ eV, is obviously insufficient to meet the resonance condition. When the sample gets closer, however, the (approximately weighted) average dielectric constant ϵ_{eff} of the space outside the metallic probe becomes larger, lowering the plasmon resonance in proportion[1] to $\epsilon_{\text{eff}}^{-1}$. As a result, the entire set of dispersion curves shifts downward, branches 3 and 4 probably moving faster than 1 and 2 since the protrusion is closer to the sample surface. When P passes through the line $\hbar\omega_l$ the resonance condition can be met by proper angular adjustment, i.e. k adjustment, of the incident radiation. According to our experimental data, this condition is satisfied best for $\theta = 74°$–$80°$ corresponding to a region close to Q in Fig. 1(b).

The increase of ϵ_{eff} and hence decrease of resonance frequency becomes significant only when the sample penetrates the near-field range of the relevant plasmon. For a spherical particle with radius R and the lowest-order, dipolelike mode, for instance,[12] this range is $\simeq 0.12R$. The shift in resonance was calculated quantitatively by Ruppin[13] who finds a dramatic decrease for $z/R < 0.3$. The diameters of the probe spheres hence will be just a few percent smaller than the positions of respective data points measured from the extrapolated origin at -220 nm. The diameters determined in this way range from 30 to 180 nm, centered roughly around 100 nm (the distribution of Δz in Fig. 3 is somewhat misleading as probes providing sharp peaks were preferred for investigation).

The distribution in size roughly agrees with the specifications of the polystyrene spheres employed if one assumes that the largest particles might represent small agglomerations of spheres while the smallest ones might be pure gold particles, possibly scratched off the film during accidental collisions with the sample. The rapid variation of ϵ_{eff} with distance[13] also may explain the narrow width of the peaks and its decrease for small particle size.

Particles with $2R < 60$ nm ($\Delta z < -160$ nm) may be considered to be within the Rayleigh limit $2R \ll \lambda$, where λ is the wavelength of the radiation near the tip. Within this limit the particle can be considered an oscillating dipole whose radiation versus size relation can be readily calculated.[14] It is also possible to scale the reduction of resonance frequency during approach with R in this case.[13] Application of the respective equations yields the curves in Fig. 3, with origin on the Δz scale, form factor of the protrusion,[14] and scaling factors for the ordinates

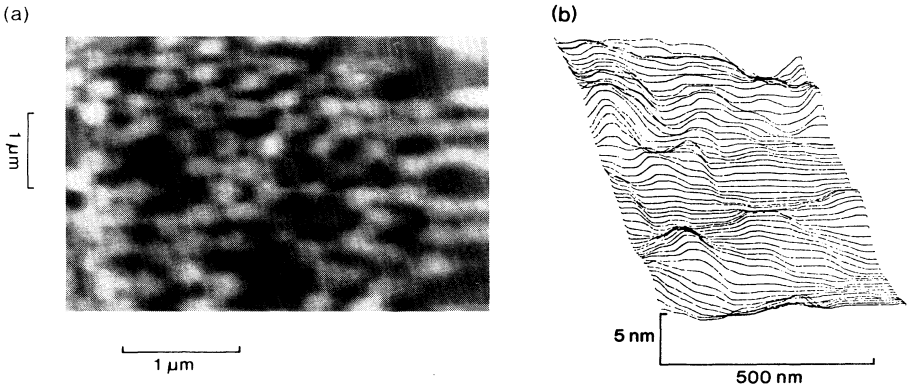

FIG. 4. SNOM images with protrusion probe: (a) Ta/W film with closely spaced holes of nominally 320 nm diameter, constant-distance mode, observation in reflection (from Ref. 9); (b) topography of a SiO_2 film (5 nm thickness) with closely spaced holes of nominally 490 nm diameter, constant-intensity mode.

as adjustable parameters. The resulting functional dependence agrees well with the experimental data within the above limit. For larger values the radiation efficiency of such particles is much less than the Rayleigh value because of the excitation of higher-order modes and other complications,[15] in qualitative agreement with our results.

Particles which provide approach curves with highly reproducible resonance peaks I_s^{peak} are excellently suited as "tips" for SNOM. Figure 4(a) shows an optical image of a thin metal film with 320-nm-diam holes, obtained with probes providing approach curves of the type shown in Fig. 2(a), operated in the constant-distance mode (tunnel distance regulation[5,9]). The resolution is ~ 50 nm, comparable to previous results from scanned aperture microscopy and the size of the protrusion used. We also were able to operate the SNOM in a topographic mode, employing an electronic control circuit which regulates the z position of the sample to provide constant I_s during scanning, in strict analogy to the generally used constant-current mode in STM *(optical tunnel microscopy)*. Figure 4(b) shows the topographic image of a glass surface covered with a 5-nm-thick SiO_2 film with closely spaced holes, nominally 490 nm in diameter. Although not optimized for this mode of operation, the recorded systematic variations in height of about 5 mm are readily associated with the somewhat irregular elevations of the iterstices between the holes.

In summary, the SNOM method allows the study of optical effects associated with individual nanometer-size particles or protrusions, in particular SP. This may open a way towards the better understanding and control of "submicroscopic" optical phenomena in general. With regard to SNOM, SP excitation adds a new dimension to detection sensitivity while the tiplike probe antenna facilitates approach to the sample surface, an important consideration for practical applications.

The authors wish to acknowledge helpful discussions with U. Dürig and technical support by J. Czaka.

[a]Address for correspondence.

[1]See, e.g., H. Raether, *Surface Plasmons on Smooth and Rough Surfaces and on Gratings,* Springer Tracts in Modern Physics Vol. 111 (Springer-Verlag, Berlin, 1988).

[2]See, e.g., *Surface-Enhanced Raman Scattering,* edited by R. K. Chang and T. P. Furtak (Plenum, New York, 1982).

[3]G. Binnig and H. Rohrer, Physica (Amsterdam) **127B**, 37–45 (1984).

[4]D. W. Pohl, W. Denk, and M. Lanz, Appl. Phys. Lett. **44**, 651 (1984); D. W. Pohl, W. Denk, and U. Dürig, Proc. SPIE **565**, 56 (1985).

[5]U. Dürig, D. W. Pohl, and F. Rohner, J. Appl. Phys. **59**, 3318 (1986).

[6]U. Ch. Fischer, J. Vac. Sci. Technol. B **3**, 386 (1985), and J. Opt. Soc. Am. B **3**, 1239 (1986).

[7]E. Betzig, A. Harootunian, M. Isaacson, and E. Kratschmer, Biophys. J. **49**, 269 (1986); A. Harootunian, E. Betzig, M. Isaacson, and A. Lewis, Appl. Phys. Lett. **49**, 674 (1986).

[8]E. Betzig, M. Isaacson, and A. Lewis, Appl. Phys. Lett. **51**, 2088 (1987).

[9]U. Ch. Fischer, U. T. Dürig, and D. W. Pohl, Appl. Phys. Lett. **52**, 249 (1988); D. W. Pohl, U. Ch. Fischer, and U. T. Dürig, Proc. SPIE **897**, 84 (1988).

[10]J. Wessel, J. Opt. Soc. Am. B **2**, 1538 (1985).

[11]D. Pohl, to be published. (Continuation of the signal beyond the kink consequently would represent the influence either of probe deformation or of the increased dielectric constant of the water-filled gap.)

[12]U. Ch. Fischer, U. T. Dürig, and D. W. Pohl, in Proceedings of the 1988 Conference on Scanning Microscopy, St. Louis, Missouri, 1988 (to be published).

[13]R. Ruppin, Surf. Sci. **127**, 108 (1983).

[14]A. Wokaun, J. P. Gordon, and P. F. Liao, Phys. Rev. Lett. **48**, 957 (1982).

[15]M. Meier, A. Wokaun, and P. F. Liao, J. Opt. Soc. Am. B **2**, 931 (1985).

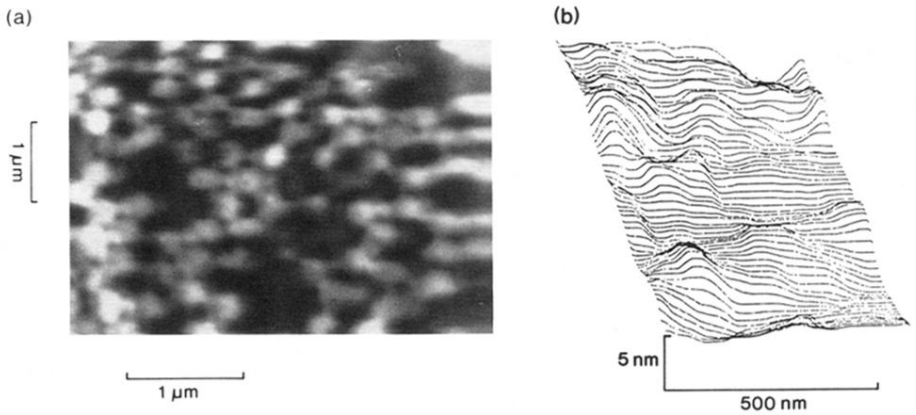

FIG. 4. SNOM images with protrusion probe: (a) Ta/W film with closely spaced holes of nominally 320 nm diameter, constant-distance mode, observation in reflection (from Ref. 9); (b) topography of a SiO_2 film (5 nm thickness) with closely spaced holes of nominally 490 nm diameter, constant-intensity mode.